Preprints (www.preprints.org) | NOT PEER-REVIEWED | Posted: 12 October 2020

Synergetic kinetics of free radical and cationic photopolymerization in three co-initiators and two-monomers system

. **Jui-Teng Lin *[1], Shaohui Liu [2,3] Pu Xiao[4] and Jacques Lalevee [2,3,*]**

. [1] New Vision Inc., 10F, No. 55, Sect.3, Xinbei Blvd, Xinzhuang, New Taipei City, Taiwan; jtlin55@gmail.com

. [2] Université de Haute-Alsace, CNRS, IS2M UMR 7361, F-68100 Mulhouse, France; shaohui.liu@uha.fr; jacques.lalevee@uha.fr.

. [3] Université de Strasbourg, France.

. [4] Research School of Chemistry, Australian National University, Camberra, ACT 2601, Australia; pu.xiao@anu.edu.au

.

. * Correspondence: jtlin55@gmail.com ; tel 8860961306877 ; and jacques.lalevee@uha.fr; Tel.: +33 3 89 60 88 03

Abstract: The synergetic features of a three-component photoinitiating systems (A/B/C) based on the measured data and proposed mechanism of Liu et al (Polymers, 2020, 12(6), 1394) are analyzed. The co-initiators/additives B and C have dual functions of : (i) regeneration of photoinitiator A and (ii) generation of extra radicals. The synergic effects lead to higher conversion of free radical polymerization (FRP) and cationic polymerization (CP). The key factors and rate constants influencing the conversion efficacy are explored by analytic formulas. Enhancing strategies for various photopolymerization systems are summarized including one component (or monomer) and one-wavelength, two-component and one, two and three-wavelength, and three-component, one-wavelength system. The synergetic effects for higher monomer conversion can be achieved by co-initiators for extra radicals and multiple wavelengths for reduced oxygen-inhibition. Co-initiator B, however, might also reduces the CP radical produced by initiator C. The conversion rate of FRP is proportional to the square root of the light intensity (I), absorption (b) and the initiator initial concentratios (A_0, B_0, C_0), whereas CP is proportional to the linear power of a parameter defined as $P=bIA_0C_0$, a stronger dependence than FRP. The CP conversion is governed by a steady-state value proportional to P, and a rate fucntion defining the depletion rate of [A][C], or the increasing rate of the conversion profile. The measured results of Liu et al (Polymers, 2020, 12(6), 1394) are well analyzed and matching the predicted features of our modeling. The specific systems analyzed are: benzophenone derivatives (A) ethyl 4-(dimethylamino)benzoate (B), and (4-tert-butylphenyl)iodonium hexafluorophosphate (C) under a UV (365 nm) LED irradiation; and monomers of trimethylolpropane triacrylate (TMPTA, for FRP) and (3,4- epoxycyclohexane)methyl 3,4-epoxycyclohexylcarboxylate (EPOX, for CP).

Keywords: polymerization kinetics; photoinitiator; monomer conversion profile; synergetic effects.

1. Introduction

Comparing to the conventional thermal-initiated polymerization, there are several advantages for photopolymerization such as fast and controllable reaction rates, and spatial and temporal control over the formation of the material, without the need for high temperatures or harsh conditions [1]. Photopolymerizations using various light with wavelength in UV, visible and near IR have been studied for both industrial and medical applications. Variety of photoresponsive materials such as conjugated polymers have been reported for additive manufacturing (AM) and recently for 3D and 4 D bioprinting [3-11]. Both spatial and temporal controlled 3D processes were reported using single and multiple wavelength lights. For 3D photo printings, the key factors include polymerization

© 2020 by the author(s). Distributed under a Creative Commons CC BY license.

Preprints (www.preprints.org) | NOT PEER-REVIEWED | Posted: 12 October 2020

depth, resolution precision and speed, in which the monomer conversion efficacy could be improved by various strategies. The reported conversion enhancing methods include the use of novel materials as enhancers or co initiators in both single and multiple components [5-8]. Two stage polymerization under two wavelengths to eliminate the oxygen inhibition effects was also reported experimentally [9-11]. Sequential network formation has also been achieved with many different types of polymerization methods, such as thiol–Michael/acrylate hybrid, epoxy/acrylate curable resins, thiol–acrylate/thiol–acetoacetate thermosets, and thiol–ene/epoxy-based polymers [12-14].

UV light (at 365 nm) have been commonly used in most type-I photoinitiators for the photopolymerization of (meth)acrylate monomers [1-3]. However, the UV wavelength suffers the disadvantages of being unsafe to skin and eyes, small penetration depth and larger light scattering in tissues [1]. Camphorquinone (CQ), due to its good visible absorption properties, is the most common type-II PI for the polymerization of (meth)acrylates under visible light [15,16].

In comparison, near-infrared (NIR) light offers advantages of safer, less light diffusion and scattering, and deeper penetration into the materials. Thus, the curing of a thick and filled material can be potentially enhanced compared to curing with UV or visible light. However, the use of NIR photoinitiating systems such as cyanine is often associated with a low reactivity and requires a high light intensity [17]. Phthalocyanines, conjugated macrocycles, have been used as commercial pigments and dyes having a high molar absorptivity coefficient in the red and NIR wavelength of 650-810 nm. Efficient polymerization conversions using NIR photoinitiation by cyanine/iodonium salt couples are reported by Schmitz et al [17]. Recently, Bonardi et al [18] reported the first three-initiator system for high performance NIR (785 nm) photopolymerization of thick methacrylates, in which (i) a borate dye used as a NIR photosensitizer (PS), (ii) an iodonium salt as a photoinitiator (PI) for the free radical polymerization of the (meth)acrylates, and (iii) a dual-function enhancer (phosphine) to prevent oxygen inhibition, and to regenerate the PS upon irradiation, in which a stable radical is coupled with the enhancer. The 3-initiator system with a dye as a photosensitizer absorbing in the NIR range, an iodonium salt (as an initiator), and a phosphine (as a co-initiator) was reported, in which the phosphine is used to reduce oxygen inhibition (OIH) during the free radical polymerization of (meth)acrylate monomers [18].

Oxygen-inhibition plays a critical role specially for optically-thin polymers. Various strategies to reduce oxygen inhibition in photoinduced polymerization have been proposed such as: (i) using a higher photoinitiator concentration; (ii) using a higher light dose or intensity, (iii) using co-initiators, (iv) addition of oxygen scavengers, and (v) working in an inert environment [19]. Besides the above methods, chemical mechanisms were also reported, such as the thiol-ene and thiol-acrylate-Michael systems which are insensitive to oxygen [8,9]. Additive enhancer-monomer were proposed to improve the curing (crosslink) efficacy by either reducing the oxygen inhibition effect by stable-monomer, or increase the lifetime of radicals in clinical applications. Dual-wavelength (red and UV) photopolymerization was also reported, in which pre-irradiation of the red light eliminated the oxygen inhibition effect and thus enhanced the conversion efficacy of the UV light [10].

Camphorquinone (CQ), due to its good visible absorption properties, is the most common type-II PI free radical photopolymerization of (meth-) acrylates under blue light [15,19]. The classical diaryliodonium salts, such as diaryliodonium, suffer low solubility in monomers and formation of side products due to the release of HF. To overcome this drawback, Kirschner et al. [15] recently reported a new counter anion-free and fluoride-free aryliodonium ylides (AY) to avoid the formation of HF and to enhance their solubility. They reported (CQ)/amine/AY as a new and efficient PI system for the polymerization of methacrylates under air and blue light (477 nm) irradiation. Kirschner et al. [15] also reported the chemical mechanisms involved in the presence of various AY and amines which lead to additional reactions and initiating radicals for improved conversion efficacy.

Example of blue and UV dual-wavelength system (without the red-light) for enhanced conversion by reducing the oxygen inhibition was reported by de Beer et al [8] and van der Laan et al [9], in which a blue (470 nm) and a UV (365 nm) light were used for the photopolymerization of methacrylate formulated with camphorquinone (CQ) and ethyl 4-(dimethylamino)benzoate (EDAB), where CQ is the blue-light active initiator (A), butyl nitrite (BN) is the UV-activated initiator (B), and

Preprints (www.preprints.org) | NOT PEER-REVIEWED | Posted: 12 October 2020

EDAB is a co-initiator (or donor D). The photochemical decomposition of BN results in the formation of nitric oxide (N), an efficient inhibitor of radical-mediated polymerizations, and alkoxide radical (X) for extra polymerization initiation, besides the initiation radical (R) generated from the blue-light

Example of 2-wavelength (red and UV) system (without the blue-light) for 3D printing was reported by Childress et al [10], in which a monomer of ethyl ether acrylate (DEGEEA) mixed by zinc 2,9,16,23-tetra-tert-butyl-29H,31H-phthalocyanine (ZnTTP) as an initiator under a UV-light, where ZnTTP/DEGEEA has distinct absorption peak at UV-365 nm and red-635 nm, respectively, and thus it can be independently excited by a UV and a red light, respectively. Lin et al [19] reported the theoretical modeling for the above described 2-wavelength system [13]. The novel strategy using 3–wavelength of uv, blue and red lights was recently proposed by Lin et al [21] theoretically for future experimental studies.

Table 1 summarizes various reported enhancing strategies for photopolymerization including one component (or monomer) and one-wavelength [15-18,22], two-component and one, two and three-wavelength [9-12,14,19-21] and three-component, one-wavelength system [13]. We note that all these systems have been theoretically and experimentally studied, except the 3–wavelength systems which was recently proposed theoretically by Lin et al [21]. The synergetic effects lead to higher monomer conversion can be achieved by co-initiators extra radicals and multiple wavelengths for reduced oxygen-inhibition. Greater details for 3-initiator and 2-monomer systems will be discussed in the next section.

Table 1. Summary of enhancing strategies for photopolymerization

System	light	Enhancer	References
one-component		co-initiators	
	blue (477 nm)	CQ/EDB/AY	Kirschner et al. [15]
	UV (365 nm)	BP/EDB/Iod	Liu et al [22]
	green (532 nm)	CQ/rose-Bengal	Wertheimer et al [16]
	NIR (785 nm)	phosphine/Iod	Schmitz et al [17].
			Bonardi et al [18]
two-component		co-monomers	
	UV (365 nm)	thiol–Vinyl (Michael)	Claudino et al [12]
		thiol–Ene	Chen et al [14]
	dual (365 + 660 nm)	DEGEEA/ZnTTP	van der Laan et al [9]
			Childress [10]
			Lin et al [19]
	Dual (365 + 430 nm)	DEGEEA/ZnTTP	Scott et al [11]
			Lin et al [20]
	3-wave (365,430, 660)	DEGEEA/ZnTTP	Lin et al [21]
three-component	UV (365 nm)	Thiol BMP/EVS/BA	Huang et al [13]

* CQ=Camphorquinone, AY=aryliodonium ylides, EDB=ethyl 4-(dimethylamino)benzoate; Iod= (4-*tert*-butylphenyl)iodonium hexafluorophosphate; BP=benzophenone; DEGEEA=ethyl ether acrylate, ZnTTP=zinc 2,9,16,23-tetra-tert-butyl-29H,31H-phthalocyanine; BMP=1-butyl mercaptopropionate; EVS=ethyl vinyl sulfone; BA= 1-butyl acrylate.

This article will present, for the first time, the kinetics of the synergetic features of the 3-initiator, [A], [B] and [C], system based on the measured data and proposed mechanism of Liu et al [22], The co-initiator [B] and [C] have dual functions of: (i) regeneration of initiator [A]; and (ii) generation of

Preprints (www.preprints.org) | NOT PEER-REVIEWED | Posted: 12 October 2020

extra radicals. The synergetic effects lead to higher conversion for FRP and CP. The key factors and rate constants influencing the conversion efficacy will be explored by analytic formulas of the conversion rate functions, derived from a kinetic model for a 3-initiator and 2-monomer system.

2. Methods and Modeling Systems

2.1. Photochemical Kinetics

As shown by Figure 1, a 3-initiator system (A/B/C) defined by the ground state of initiator-A, which is excited to its first-excited state PI*, and a triplet excited state T by a quantum yield (q). The triplet state T interacts with initiator [A] and [B] to produce radical R; and interacts with co-initiator [C] to produce radical S'and S; in which the coupling of the radicals R with [C] and S' with [B] lead to the regeneration of [A]. Radicals S and S' are responsible, respectively, for the free radical polymerization (FRP) and cationic polymerization (CP), via monomers M and M'. For system with [A] alone, T, R' and R could be responsible for FRP, in general. For CP, Figre 1 also includes the coupling of S'and M' to produce a propagating cation (Q), which could couple with [B] for a termination. In general, the terminations of our proposed scheme include the couplings of R+R (bimolecule), R+R', (T,R,S) + M (for FRP); S'+M' and [B]+Q (for CP). We will show later that Figure 1 is more general than the proposed Scheme of Liu et al [22].

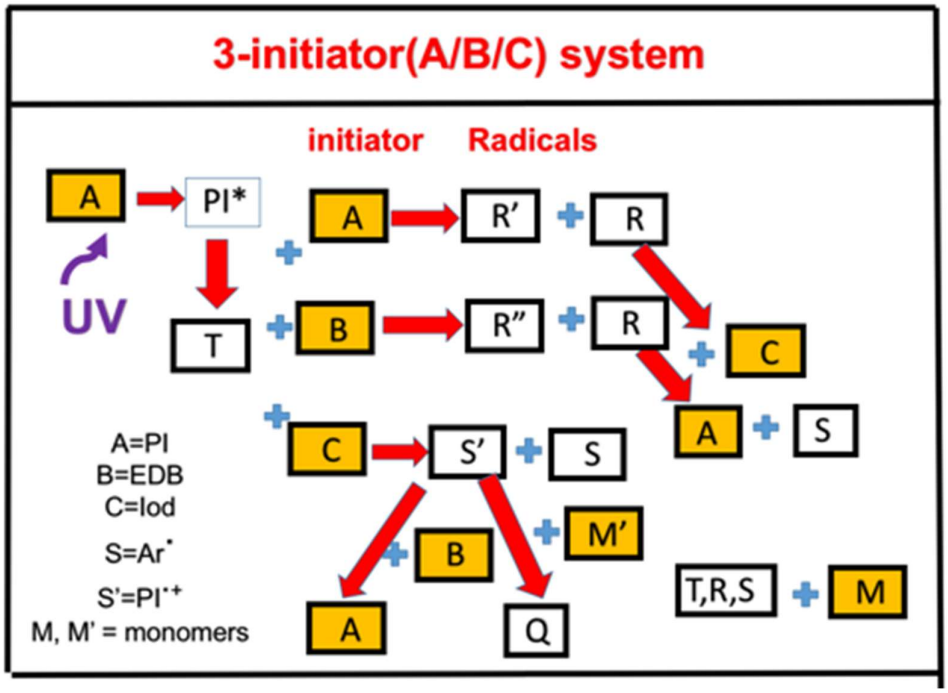

Figure 1. The schematics of a 3-initiator system, (A/B/C), where A is the ground state initiator, having a first excited state PI*, and a triplet state T, which interacts with initiator [A] and [B] to produce radical R; and interacts with initiator [C] to produce radical S, in which the coupling of the radical R with [C] and S'with [B] could lead to the regeneration of [A].

A specific system reported by Liu et al [22] is shown by the mechanism of Figure 2, where [A] is benzophenone (BP) photoinitiator, co-initiator [B] is ethyl 4-(dimethylamino)benzoate (EDB), and [C] is (4-*tert*-butylphenyl)iodonium hexafluorophosphate (Iod). Under a UV (365 nm) LED irradiation, [A] transforms from ground state (PI) to excited triple state ^{1,3}PI (shown by r1). For BP alone, PI-H$^{\bullet}$ (or R) and PI(-H)$^{\bullet}$ (or R') are the active species for FRP (shown by r2). In the presence of EDB, extra radical PI-H$^{\bullet}$ is produced (shown by r3) and could couple with [C] to produce aryl radical Ar$^{\bullet}$ and

Preprints (www.preprints.org) | NOT PEER-REVIEWED | Posted: 12 October 2020

cation $PI^{\bullet+}$ which lead to FRP and CP, respectively (shown by r5). Associated with the photolysis of BPC1/Iod and BPC1/EDB/Iod, the photoredox catalytic cycle was proposed in three-component PI/EDB/Iod system (shown by r5 and r6). The regeneration of PI speeds up the photopolymerization and slows down the consumption of PI in the photolysis experiments. Trimethylolpropane triacrylate (TMPTA) and (3,4- epoxycyclohexane)methyl 3,4-epoxycyclohexylcarboxylate (EPOX) were used as benchmark monomers for FRP and CP, respectively.

However, we note that our Figure 1 is more general than the following Scheme of Liu et al [22] which ignored the coupling of $PI^{\bullet+}$ and epoxy monomer producing a propagating cation (Q) which could be terminated by [B] as cationic polymerizations were not experimentaly carried out in presence of B due to its inhibitor effect. Furthermore, the measured data of Liu et al [22] for the case of CP was limitd to two initiators of [A] and [C], although 3-initiator systems of [A]/[B]/[C] was studied in FRP. Our modled system of Figure 1 and the associated kinetic equations to be shown later include 3-initiator for both FRP and CP.

$$PI \xrightarrow{h\nu} {}^{1,3}PI \qquad (r1)$$

$${}^{1,3}PI + PI \longrightarrow PI^{\bullet-} + PI^{\bullet+} \longrightarrow PI\text{-}H^{\bullet} + PI_{(-H)}{}^{\bullet} \qquad (r2)$$

$${}^{1,3}PI + EDB \longrightarrow PI^{\bullet-} + EDB^{\bullet+} \longrightarrow PI\text{-}H^{\bullet} + EDB_{(-H)}{}^{\bullet} \qquad (r3)$$

$${}^{1,3}PI + Ar_2I^{+} \longrightarrow PI^{\bullet+} + Ar_2I^{\bullet} \longrightarrow PI^{\bullet+} + Ar^{\bullet} + ArI \qquad (r4)$$

$$PI\text{-}H^{\bullet} + Ar_2I^{+} \longrightarrow PI + Ar^{\bullet} + ArI + H^{+} \qquad (r5)$$

$$PI^{\bullet+} + EDB \longrightarrow PI + EDB^{\bullet+} \qquad (r6)$$

Figure 2. The mechanism of a 3–initiator and 2-monomer, A/B/C/M/M'system proposed by Liu et al [22].

The kinetic equations for our previous 2-initiator and 1-monomer system [23-25] are revised for the 3-initiator and 2-monomer system, A/B/C/M/M', as follows

$$\frac{\partial[A]}{\partial t} = -bI(z,t)[A] - k_1T[A] + R_E \qquad (1)$$

$$\frac{\partial[B]}{\partial t} = -(k_2T + k_7S' + k_{10}Q)[B] \qquad (2)$$

$$\frac{\partial[C]}{\partial t} = -(k_3T + k_6R)[C] \qquad (3)$$

$$\frac{\partial T}{\partial t} = bI(z,t)[A] - (k_5 + k_1[A] + k_2[B] + k_3[C] + k_8M)T \qquad (4)$$

$$\frac{\partial R}{\partial t} = (k_1[A] + k_2[B])T - (k_6[C] + k_9M)R \qquad (5)$$

$$\frac{\partial S}{\partial t} = k_3T[C] + k_6R[C] - 2k_TS^2 - KSM \qquad (6)$$

$$\frac{\partial S'}{\partial t} = k_3T[C] - k_7[B]S' - K'S'M' \qquad (7)$$

$$\frac{\partial Q}{\partial t} = K'S'M' - k_{10}[B]Q \qquad (8)$$

where $R_E = k_5T + k_6R[C] + k_7S'[B]$ is the regeneration term of of [A]. $b = 83.6a'wq$, where w is the UV light wavelength (in cm) and q is the triplet state T quantum yield; a' is the mole absorption

Preprints (www.preprints.org) | NOT PEER-REVIEWED | Posted: 12 October 2020

coefficient, in (1/mM/%) and I (z, t) is the light intensity, in mW/cm^2. All the rate constants are defined previously and they are related by the coupling terms. For examples, k_j (with j=1,2,3) are for the couplings of T and [A], [B], and [C], respectively; k_6 and k_7 are for the couplings of R and [C], and S′ and [B], respectively; and k_T is the bimolecular termination rate of S. The coupling among T,R, S, and S and M (M′) for polymerization are given by k_8, k_{89}, K and K′, respectively.

The monomers conversions are given by [23]

$$\frac{dM}{dt} = -(KS+k_8T+k_9R)M \quad (9)$$

$$\frac{dM'}{dt} = -K'S'M \quad (10)$$

For FRP and CP, given by the interaction of (T,R,S) and M, and S′ and M′, respectively.

We note that Eq. (1) to (10) are constructed for the specific system of Liu et al [22], in which the following couplings (or effects) are ignore: oxygen inhibition, couplings of S and S′, R and S, R and [B], R and [A], S′ and [A]; and the direct coupling of initiators, [A], [B], [C] and the monomers, M and M′ (type-I processes). For [A] alone, we assume the FRP is mainly due to T and R, and the coupling of R′ and M is ignored.We also limit the FRP is dominated by the bimolecular termination of S, whereas CP is dominated by the unimolecular termination of S′. More comlex systems including above couplings and the oxygen inhibition effects have been reported by Lin et al [25].

For comprehensive modeling we will use the so-called quasi-steady state assumption [15,18]. The life time of the singlet and triplet states of photosensitizer, the radicals (R, S and S′), since they either decay or react with cellular matrix immediately after they are created. Thus, one may set dT/dt=dR/dt=dS′/dt=dQ/dt=0, which give the quasi-steady-state solutions: T=bIg[A], S′= bIg[A](k_3[C]′) [C]/(k_7[B]+K′M), R= bIgg′[A], Q=K′S′M′/k_{10}[B]; g= G/(k_5+G), G=k_1[A]+k_2[B]+k_3[C]+k_8M; g′=(k_1[A]+k_2[B])/(k_6[C]+k_9M).

The kinetic Equation (8) to (12) become,

$$\frac{\partial[A]}{\partial t} = -bIg[A](1 - k_7 - k_1) + k_6R[C] \quad (11)$$

$$\frac{\partial[B]}{\partial t} = -(k_2bIg[A]+k_7S')[B] - K'S'M' \quad (12)$$

$$\frac{\partial[C]}{\partial t} = -(k_3bIg[A]+k_6R)[C] \quad (13)$$

$$\frac{\partial S}{\partial t} = (k_3bIg[A] + k_6R)[C] - 2k_TS^2 - KSM \quad (14)$$

Eq. (11) to (14) require a full computer simulation. However, the steady-state radical given by dS/dt=0, We obtain the more simplified equations as follows

$$\frac{\partial[A]}{\partial t} = -bIg(1 - k_7 - k_1 + k_3[C] + k_6g'[C])[A] \quad (15)$$

$$\frac{\partial[B]}{\partial t} = -bIg(k_2[B] + k_3[C])[A] - K'S'M' \quad (16)$$

$$\frac{\partial[C]}{\partial t} = -bI(k_3g + k_6g')[A][C] \quad (17)$$

Preprints (www.preprints.org) | NOT PEER-REVIEWED | Posted: 12 October 2020

$$\frac{dM}{dt} = -R_T M \quad (18)$$

$$\frac{dM'}{dt} = -R_T' M' \quad (19)$$

where R_T=KS +k_8bIg[A] and R'$_T$= K'k_3bIg[A][C]/ (k_7[B]+K'M). S is the steady-state solution of Eq. (14) given by S=[(0.5/k_T)bIgG']$^{0.5}$, with G'=k_1[A]+k_2[B]+k_3[C], for the case that KM<<2k_TS and k_9M<< k_6[C].

Analytic formulas for the FRP rate function is given by

$$R_T = \sqrt{bIg(\, k_8[A] + 0.5G'/k_T)} \quad (20)$$

where G'=k_1[A]+k_2[B]+k_3[C].

Similary, for the case that K'M<<k_7[B]. the CP rate function is given by

$$R'_T = K' (k_3/k_7) bIg[A][C]/[B] \quad (21)$$

For the case that k_7[B]<< K'M, we obtain

$$R'_T = k_3 bIg[A][C][1 - \frac{k_7[B]}{K'M}]/M \quad (22)$$

The conversion efficacy of monomer M and M' are defined by C_V=1- M/M_0 = 1- exp(-E), C'$_V$=1- M'/M'$_0$ = 1- exp(-E'), where the E and E' function are given by the time integral of the rate function, R_T and R'$_T$, given by Eq. (20) and (21) to define the conversion of FRP and CP, respectively. We note that there is a basic difference of the enhancing feature of FRP and CP given by Eq. (20) to (22). FRP is proportional to the square-root of bIg(k_1[A]+k_2[B]+k_3[C]) shown by Eq. (20), whereas CP is proportional to the linear power of bIg[A][C]/M, a stronger dependence than FRP.

For analytic approximated form of [A]=A_0 exp[-bI'gt], [C]=C_0 exp[-k_3bI'gA_0t), and an averaged light intensity of I' [23,24], we obtain an analytic formula of Eq. (22) and the CP conversion (C$_V$') is given by, for ignore k_7[B]<<K'M,

$$C'_V = P[\, 1 - exp(-Ht)] \quad (23)$$

with A_0 , C_0 and M_0 are the initial concentration of [A], [C] and M, respectively; P=k_3(A_0 C_0 /M_0) /(1+k_3A_0) and H= bIg(1+ k_3A_0). We note that the CP conversion profile is governed by P, for its steady-state value, and H, for the depletion rate of [A][C], or the increasing rate of the conversion profile. However, the FRP conversion is much more complex and there is no analytic formula. Numerical results based on Eq. (23) and more discussion will be shown later.

3.. Results and discussion

3.1 Synergetic effects

As shown by Figure 1, and Eqs. (20) to (23), the following synergetic features of the 3-initiator system A/B/C are summarized.

(a) Initiator [B] has multiple functions of : (i) regeneration of initiator [A] leading to higher FRP conversion; (ii) generation of radical R and S for the FRP conversion; and (iii) coupling with [C] leads to the reduction of radical S' and the CP conversion. Therefore, the competetion of (i), (ii) and (iii) defines the net enhancement or synergetic effect, in which the rate constants k_J and initial concentration of [B] play the major role. Higher [B] always leads to higher FRP conversion than that of [A] alone, as shown by Eq. (20) with G'= k_3 + (k_1[A]+k_2[B])/[C].

Preprints (www.preprints.org) | NOT PEER-REVIEWED | Posted: 12 October 2020

(b) Similarly, initiator [C] has functions of : (i) regeneration of initiator [A] to enhance the radicals R and S, leading to higher FRP conversion; (ii) generation of cationic radical S' for CP conversion; and (iii) enhancing FRP conversion by generation of radical S via the couplin of R and [C] (as shown by Figure 1). We note that [C] always enhances both FRP and CP conversions, whereas our Figure 1 shows that [B] could inhibit radical S' leading to reduced CP. However, this general feature demonstrated by Figure 1 was not explored by the work of Liu et al [22].

(c) Without [B] and [C], the FRP for [A] alone is given by the coupling of T and R with the monomer (M), or the first term of Eq. (20), $k_8 bIg$ [A], and the contribution from g'.

(d) The presence of [B] leads to efficient FRP, but it also consumes [C] and thus reduces CP, as shown by Eq. (21) and (22). Therefore, in the 2-monomer system, the dominant polymerization is FRP or CP depending on the relative concentration of [A][C] and [B] and the rate constants which define the amount of radicals S and S'.

(e) FRP conversion is proportional to the square-root of $bIg(k_1[A]+k_2[B]+k_3[C])$ *shown by Eq. (20), whereas CP conversion is proportional to the linear power of* $bIg[A][C]/M$*, a stronger dependence than FRP.*

(f) The *CP conversion is governed by* the *concentration ratio* $P=k3(A_0 C_0 /M_0) /(1+k3A_0)$ for its steady-state value, and and $H= bIg(1+ k_3A_0)$, for the depletion rate of [A][C] *and also the rising rate of the* conversion *function.*

Figure 3 shows the results based on Eq. (23) for CP conversion for various co initiator concentration ratio P and rate constant H. We note that larger P achieves the higher steady-state profile, as shown by Figure 3(A). Furthermore, the profile rising rates are given by the H values. Higher light intensity (I), larger initiator concentration, or stronger absorption (b) leads to a faster depeltion of [A] and [C] and hence faster rising of the conversion profile, shown by Figure 3(B). We note that for the same P value, the CP conversion profiles having different H-values reach the same steady state. However, we have previously reported different features of FRP [23,25] that larger H-value reaches a lower steady state conversion, as also shown by Eq. (20), which is fundamentally different from Eq. (22) and (23).

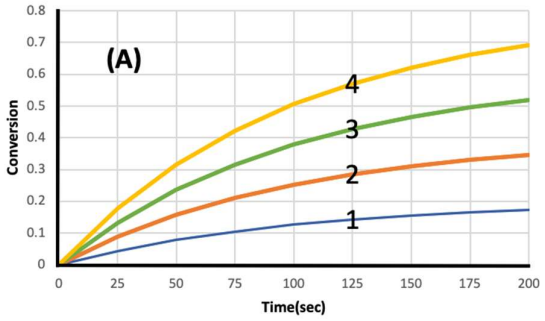

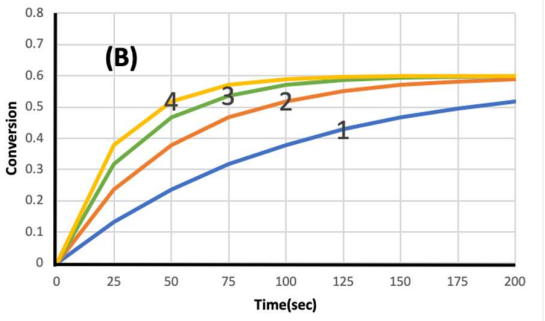

Preprints (www.preprints.org) | NOT PEER-REVIEWED | Posted: 12 October 2020

Figure 3. The calculated CP conversion profiles for various P and H values: (A) for fixed H=0.01, and P = (0.2, 0.4,0.6, 0.8), for Curves 1,2,3 and 4; (B) for fixed P=0.6, and H= (0.01, 0.02, 0.03, 0.04) for Curves 1,2,3, and 4, respectively.

3.2 Analysis of measured results

Besides the synergetic effects described in last section, our formulas shown by Eq. (18) to (23), may be used to analyze the measured results of Liu et al [22] as follows:

(a) Fig. 3 of Liu et al [22] for cationic polymerization of EPOX showed that BPC1/Iod system has the highest conversion (44%) due to its highest light absorption. The role of light absorption was shown by Eq. (22) and (23), in which the conversion rate is an increasing function of b, defined by $b=83.6a'wq$, where a' is the molar extinction coefficient, w is the UV light wavelength and q is the triplet state quantum yield. BPC1-BPC4 have higher molar extinction coefficients, therefore the CP conversion rate of EPOX for BPC1-BPC4/Iod systems are faster than C5-C8/Iod systems for the same initial concentration of PI and Iod. Fig. 3 of Liu et al [22] may be compared with our Figure 3(A), where higher P value leads to larger steady-state conversion, as also shown by Eq. (22) and (23).

(b) Fig. 4b of Liu et al [22] showed that higher FRP conversion of TMPTA in the presence of PI/EDB systems comparing to that of PI alone, shown by Fig. 4a. This enhanced polymerization is due to the increase of the conversion rate as shown by the additional term $k_2[B]$ of Eq. (20). EDB (or co initiator [B]) as H donor has an effective interaction with PI to generate radicals which promote the free radical polymerization, so the PI/EDB systems have better polymerization performance than PI alone systems.

(c) Fig. 4 d of Liu et al [22] shown that FRP conversion of TMPTA initiated by PI/EDB/Iod (or A/B/C) systems are better than PI/EDB (or A/B) and PI/Iod (or A/C) systems. This can be easily realized by our Eq. (20), that the conversion rate is an increasing function of $G'= k_1 [A]+ k_2 [B] +k_3 [C]$. That is, 3-initiator system is more efficient than that of two (with [B] or [C]=0) and one initiator (with [B]=[C]=0) systems. In PI/EDB/Iod system, the triple state (T) reacts with PI, EDB and Iod at the same time. There is a photoredox catalytic cycle in 3-initiator system and the regeneration of PI speeds up the polymerization, in additional to the free radicals (R,S and S'). Therefore, PI/EDB/Iod systems have better polymerization performances than PI/EDB and PI/Iod systems.

(d) Fig. 5 of Liu et al [22] showed that the consumption rate of BPC1 in BPC1/TEOA/Iod system was slower than BPC1/Iod system. The photoredox catalytic cycle in the three-component system could regenerate BPC1, as shown by Eq. (1) and (8).

(e) Fig. 6 and S1 of Liu et al showed that the consumption rates of BPC1-BPC4 were faster than C5 and C7 due to the presence of the benzophenone moiety in BPC1-BPC4 structures which promoted the reaction between PI and amine. The photolysis demonstrated the benzophenone-carbazole PIs had high reactivity. Higher reactivity of co-initiator benzophenone leads to higher conversion, as shown by the rate constants, k_j (with j=1,2,3) in Eq. (20).

Preprints (www.preprints.org) | NOT PEER-REVIEWED | Posted: 12 October 2020

(f) Fig. 7 of Liu et al [22] showed the fluorescent properties as the evidence of the interaction capacity of PIs with additives in the excited singlet state. The role of triple-state quantum yield (q) was also shown by the b factor of Eq. (20) and (21). The fluorescence experiments demonstrated that benzophenone-carbazole PIs could be quenched easily by additives. The high electron transfer quantum yields show that electron transfer occurs effectively between benzophenone-carbazole PIs and EDB/Iod and therefore, lead to high polymerization conversions.

5. Conclusion

Higher conversion of FRP and CP can be achieved by co-initiators via the regeneration of photoinitiator A and generation of extra radicals S and S'. The synergic effects of FRP are proportional to the square root of bIg(k_1[A]+k_2[B]+k_3[C]) shown by Eq. (20), whereas CP conversion is proportional to the linear power of bIg[A][C]/M, a stronger dependence than FRP. The CP conversion is governed by a steady-state value (P), and an H-function for the depletion rate of [A][C], or the increasing rate of the conversion profile. The measured results of Liu et al [22] are well analyzed and matching the predicted features of our modeling.

Author Contributions: Conceptualization, JTL and JL; Methodology, JTL and SL; Software, JTL; Validation, JTT; Formal Analysis, JTL; Investigation, JTL and JL; Data Curation, SL; Writing-Original Draft Preparation, JTL; Writing-Review & Editing, JTL, PX and JL; Funding Acquisition, JL.

Funding: This research was partly funded by the China Scholarship Council (CSC); grant number CSC201906880009. The Agence Nationale de la Recherche (ANR agency) is acknowledged for its financial support through the NoPerox grant.

Acknowledgments: The authors thank the assistance from Jonathan Y.K. Hu (Kaohsiung American School, Taiwan) for computer graphs. S.L thanks China Scholarship Council (CSC201906880009). JTL thanks the internal grant of New Vision Inc.

Conflicts of Interest: Jui-Teng Lin is the CEO of New Vision Inc.

References

1. Fouassier, J. P. & Lalevée, J. Photoinitiators for Polymer Synthesis-Scope, Reactivity and Efficiency. Wiley-VCH Verlag GmbH & Co. KGaA: Weinheim, Germany, 2012.
2. Yagci, Y., Jockusch, S. & Turro, N.J. Photoinitiated polymerization: Advances, challenges and opportunities. *Macromolecules* **43**, 6245–6260 (2010).
3. Ligon, S.C.; Liska, R.; Stampfl, J.; Gurr, M.; Mulhaupt, R. Polymers for 3D printing and customized additive manufacturing. *Chem. Rev.* **2017**, *117*, 10212−10290.
4. Takagishi, K.; Umezu, S. Development of the improving process for the 3D printed structure. *Sci. Rep.* **2017**, *7*, 39852.
5. Shusteff, M.; Browar, A.E.M.; Kelly, B.E.; Henriksson, J.; Weisgraber, T.H.; Panas, R.M.; Fang, N.X.; Spadaccini, C.M. One-step Volumetric Additive Manufacturing of Complex Polymer Structures. *Sci. Adv.* **2017**, *3*, 7.
6. Janusziewicz, R.; Tumbleston, J.R.; Quintanilla, A.L.; Mecham, S.J.; DeSimone, J.M. Layerless Fabrication with Continuous Liquid Interface Production. *Proc. Natl. Acad. Sci. USA* **2016**, *113*, 11703−11708.

Preprints (www.preprints.org) | NOT PEER-REVIEWED | Posted: 12 October 2020

7. Kelly, B.E.; Bhattacharya, I.; Heidari, H.; Shusteff, M.; Spadaccini, C.M.; Taylor, H.K. Volumetric Additive Manufacturing via Tomographic Reconstruction. *Science* **2019**, *363*, 1075−1079.
8. de Beer, M.P.; van der Laan, H.L.; Cole, M.A.; Whelan, R.J.; Burns, M.A.; Scott, T.F. Rapid, Continuous Additive Manufacturing by Volumetric Polymerization Inhibition Patterning. *Sci. Adv.* **2019**, *5*, 8.
9. van der Laan, H.L.; Burns, M.A.; Scott, T.F. Volumetric Photopolymerization Confinement through Dual-Wavelength Photoinitiation and Photoinhibition. *ACS Macro Lett.* **2019**, *8*, 899–904.
10. Childress, K.K., Kim, K., Glugla, D.J., Musgrave, C.B., Bowman, C.N. & Stansbury, J.W. Independent control of singlet oxygen and radical generation via irradiation of a two-color photosensitive molecule. Macromolecules **52**(13):4968–4978 (2019).
11. Scott, T.F.; Kowalski, B.A.; Sullivan, A.C.; Bowman, C.N.; McLeod, R.R. Two-Color Single-Photon Photoinitiation and Photoinhibition for Subdiffraction Photolithography. *Science* **2009**, *324*, 913–917.
12. Claudino,M.; Zhang,X.; Alim,M.D.;Podgórski,M.;Bowman, C. N. Mechanistic Kinetic Modeling of Thiol-Michael Addition Photopolymerizations via Photocaged "superbase" Generators: An Analytical Approach. Macromolecules 2016, 49 (21), 8061−8074.
13. Huang, S.; Sinha, J.; Podgorski, M.; Zhang, X.; Claudino M. Bowman, C.N. Mechanistic modeling of the Thiol−Michael addition polymerization kinetics: Structural effects of the Thiol and Vinyl monomers. *Macromolecules* **2018**, *51*, 5979–5988.
14. Chen, K.T., Cheng, D.C., Lin, J.T. Liu, H.W. Thiol-Ene photopolymerization in thick polymers: kinetics and analytic formulas for the efficacy and crosslink depth. *Polymers* **11**, 1640 (2019) doi:10.3390/polym11101640.
15. Kirschner, J., Paillard, J., Bouzrati-Zerell, M, et al. Aryliodonium ylides as novel and efficient additives for radical chemistry: example in camphorquinone (CQ)/Amine based photoinitiating systems. *Molecules* **24**(16), 2913 (2019); doi:10.3390/molecules24162913.
16. Wertheimer CM, Elhardt C, Kaminsky SM et al. Enhancing rose Bengal photosensitized protein crosslinking in the cornea. Invest. Ophthalmol Vis Sci. 2019, 60, 1845-1852.
17. Schmitz C, Halbhuber A, Keil D, Strehmel B. NIR-sensitized photoinitiated radical polymerization and proton generation with cyanines and LED arrays. Prog. Org. Coat. 2016, 100, 32−46.
18. Bonardi AH, Dumur F, Grant TM, et al. High performance near-Infrared (NIR) photoinitiating systems operating under low light intensity and in the presence of oxygen. Macromolecules, 2018, 51, 1314-1324.
19. Lin JT, Liu HW. Chen KT, Chiu YC, Cheng DC. Enhancing UV photopolymerization by a red-light pre-irradiation: kinetics and modeling strategies for reduced oxygen-inhibition. J Polymer Science, 2020，58， 683-691，DOI:10.1002/pol.20190201.
20. Lin JT, Chen KT, Cheng DC, Liu HW. Dual-wavelength (UV and Blue) controlled photopolymerization confinement for 3D-printing: modeling and analysis of measurements. Polymers, 2019, 11, 1819.

Preprints (www.preprints.org) | NOT PEER-REVIEWED | Posted: 12 October 2020

21. Lin, J.T., Liu, H.W., Chen, K.T. Cheng, D.C. 3-wavelength (UV, blue, red) controlled photopolymerization: improved conversion and confinement in 3D-printing. IEEE Access, 2020, 8, 49353-49362.
22. Liu, S.; Chen, H.; Zhang, Y.; Sun, K.; et al. Monocomponent photoinitiators based on Benzophenone-carbazole structure for LED photoinitiating systems and application on 3D printing. Polymers, 2020, *12*(6), 1394.
23. Lin, J.T,; Cheng, D.C. Modeling the efficacy profiles of UV-light activated corneal collagen crosslinking. PloS One. 2017;12:e0175002.
24. Lin, J.T. Kinetics of Enhancement for Corneal Cross-linking: Proposed Model for a Two-initiator System. Ophthalmology Research, 2019, 10(3): 1-6; Article no.OR.49970 DOI: 10.9734/OR/2019/v10i330109
25. Lin, J.T,; Chen. K.T,; Cheng. D,C,; Liu. H,W. Modeling the efficacy of radical-mediated photopolymerization: the role of oxygen inhibition, viscosity and induction time. *Front. Chem.2019, 7:760. doi: 10.3389/fchem.2019.00760.*